



**CIRRELT**

Centre interuniversitaire de recherche  
sur les réseaux d'entreprise, la logistique et le transport

Interuniversity Research Centre  
on Enterprise Networks, Logistics and Transportation

---

# Midterm Hydro Generation Scheduling Under Uncertainty Using the Progressive Hedging Algorithm

Pierre-Luc Carpentier  
Michel Gendreau  
Fabian Bastin

July 2012

CIRRELT-2012-35

**Bureaux de Montréal :**

Université de Montréal  
C.P. 6128, succ. Centre-ville  
Montréal (Québec)  
Canada H3C 3J7  
Téléphone : 514 343-7575  
Télécopie : 514 343-7121

**Bureaux de Québec :**

Université Laval  
2325, de la Terrasse, bureau 2642  
Québec (Québec)  
Canada G1V 0A6  
Téléphone : 418 656-2073  
Télécopie : 418 656-2624

[www.cirrelt.ca](http://www.cirrelt.ca)

# Midterm Hydro Generation Scheduling Under Uncertainty Using the Progressive Hedging Algorithm

Pierre-Luc Carpentier<sup>1,2,\*</sup>, Michel Gendreau<sup>1,2</sup>, Fabian Bastin<sup>1,3</sup>

<sup>1</sup> Interuniversity Research Centre on Enterprise Networks, Logistics and Transportation (CIRRELT)

<sup>2</sup> Department of Mathematics and Industrial Engineering, École Polytechnique de Montréal, P.O. Box 6079, Station Centre-ville, Montréal, Canada H3C 3A7

<sup>3</sup> Department of Computer Science and Operations Research, Université de Montréal, P.O. Box 6128, Station Centre-Ville, Montréal, Canada H3C 3J7

**Abstract.** We assess the applicability of the progressive hedging algorithm (PHA) for solving Hydro-Québec's (HQ) midterm hydro generation scheduling problem (MGSP). This optimization problem is formulated as a large-scale multistage stochastic linear program (MSLP) for which decisions are distributed over an extended planning horizon with weekly time steps. A discretized load duration curve is used to represent short-term load variations at each time period. Natural inflow variability is represented by a finite scenario tree. Other input parameters are assumed to be deterministic. Power output of variable-head hydro plants is represented using concave and piecewise linear functions, which depend on water release and upstream and downstream reservoir levels. Reservoir dynamics, energy balance and transmission network constraints are also included in the model. The proposed model is tested on HQ power system using realistic data. Computational results show that the penalty parameter must be chosen carefully to minimize the algorithm's running time without sacrificing solution quality. In general, the PHA converges rapidly to a poor solution when the penalty parameter is too large. Conversely, a large number of iterations is required to satisfy non-anticipativity constraints when penalization is too weak. For this problem, updating the penalty parameter at each iteration is necessary to obtain a high quality solution in reasonable time.

**Keywords:** Midterm hydro scheduling, multistage stochastic linear program, progressive hedging algorithm, scenario decomposition, multireservoir system operation, hydropower.

**Acknowledgements.** The authors would like to express their gratitude to Hydro-Québec, the Natural Sciences and Engineering Research Council of Canada (NSERC) and Fonds de recherche du Québec – Nature et technologies (FRQNT) for their financial support.

Results and views expressed in this publication are the sole responsibility of the authors and do not necessarily reflect those of CIRRELT.

Les résultats et opinions contenus dans cette publication ne reflètent pas nécessairement la position du CIRRELT et n'engagent pas sa responsabilité.

---

\* Corresponding author: Pierre-Luc.Carpentier@cirrelt.ca

## 1. Introduction

Hydro-Québec's (HQ) is the main electric utility in Québec, Canada. The company operates, mostly, hydroelectric power plants with large storage capacity to meet Québec's domestic load. In this study, we consider the midterm generation scheduling problem (MGSP) which is solved on a weekly basis by HQ's system managers. The aim of this problem is to find optimal water release targets and reservoir state trajectories over the coming years to maximize efficiency. Reservoir level must be managed carefully to ensure that HQ's system has enough available power and stored energy to meet the domestic load efficiently at all time.

In Québec, interannual and seasonal variability of reservoir inflows is large as shown in Fig. 1. Seasonal cycles for load and reservoir inflows have a large amplitude and are out of phase by a few months. The peak load period occurs during mid-winter (January-February) when the reservoir inflows reaches its lowest intensity. Reservoirs are replenished a few months later during the spring flood (May-July) as the snow melts and the electrical load is much lower. At the multi-annual time scale, water must be stored during wet years in order to meet the load during dry years.

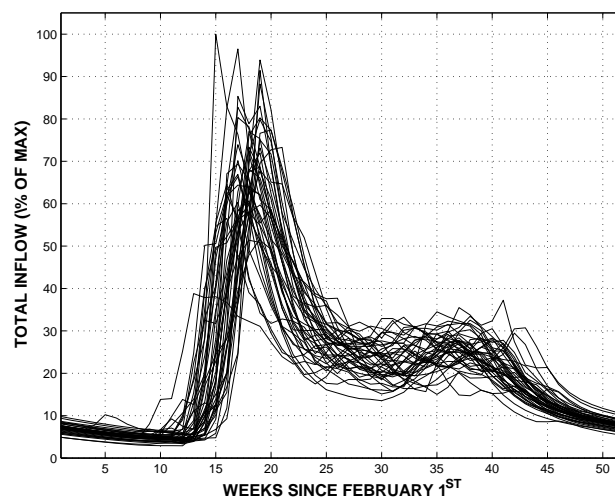


Figure 1: Seasonal cycle of total reservoir inflows for 42 years of historical record.

The current decision support system (DSS) used by Hydro-Québec managers is based on a deterministic optimization model returning a detailed production plan for the coming 78–104 weeks (periods). The model takes into account reservoir dynamics, head variations, turbine efficiency curves and transmission network constraints. However, potential sources of uncertainty on input parameters (e.g. inflows, load, failures, ...) are neglected in the deterministic model. In practice, managers run their deterministic model using different inflow scenarios (e.g. wet, dry, average). Robust solutions are obtained by adding experience-based

restrictions (bounds) on reservoir release and storage at specific time periods.

The company is currently studying alternative approaches to incorporate reservoir inflows uncertainty explicitly within a new stochastic optimization model. Doing so would hopefully increase the quality of solutions returned by the DSS and simplify the manager's task by reducing the necessity of relying on experience-based restrictions. Uncertainty modeling in multistage problems increases dramatically the size of the optimization problem to be solved. Sophisticated solution methods must be employed to solve efficiently this problem with reasonable computing resources ( $< 1$  hour on a PC).

Reservoir management problems under inflow uncertainty were studied extensively over the past decades. Comprehensive literature reviews can be found in [1], [2], [3] and [4]. The most common approach for solving efficiently this class of problem relies on the dynamic programming (DP) principle [5] and consists in applying time decomposition on the original problem. Instead of solving directly the (large) multistage stochastic program, the approach consists in solving a sequence of (small) subproblems. Each subproblem is associated to a specific time period of the planning horizon and a possible state of the dynamic system. DP-based methods were applied repeatedly for reservoir management problems in the literature [6] and [7]. Discrete stochastic DP (SDP) was applied in reservoir management problem [8]. Unfortunately, this exact method is limited to systems with two reservoirs or less due to the so-called *curse of dimensionality*. Due to this phenomenon, the computational complexity of the SDP algorithm grows exponentially with the dimension of state and control vectors.

Different approximate DP (ADP) methods were developed to mitigate dimensionality problems in DP [9]. One possible approach to reduce the size of state and control spaces is to aggregate many reservoirs into a larger hypothetical reservoir and apply SDP over the resulting system. This type of approach was applied for large reservoir systems [10] and [11]. The neuro-DP (NDP) algorithm [12] is a promising ADP approach to extend the applicability of discrete SDP. The state space dimensionality problem is mitigated by reducing the number states for which subproblems are solved. Approximate values of the Bellman function for unsampled states are obtained by interpolation using an artificial neural network. Castelletti *et al.* [13] applied the NDP algorithm on a three-reservoir system. Their results suggest this method is applicable for systems with more than three reservoirs. However, it is unlikely that this method could be applicable for large hydroelectric power systems (20 reservoirs or more). The stochastic dual DP (SDDP) algorithm [14] is another type of ADP method which was used extensively for management of large multireservoir systems [15], [16], [17], [18] and [19]. With this method, the *curse of dimensionality* associated with state and control spaces is avoided since the method is based on continuous spaces. The nested Benders decomposition algorithm is another approach which was applied for large reservoir systems [20] and [21].

If reservoir inflows variability is modeled using a scenario tree, the progressive hedging algorithm (PHA) proposed by Rockafellar and Wets [22] is a promising alternative to

DP-based methods. With this approach, each subproblem is associated with a particular scenario in the tree. Santos *et al.* [23] Gonçalves *et al.* [24] applied the PHA for a midterm planning problem of the Brazilian system over a 6–7 period planning horizon. Their results show that the PHA is competitive with the nested Benders decomposition method for this problem.

This paper proposes a new stochastic optimization model to solve HQ’s scheduling problem over a 78–104 periods (weeks) horizon. Aggregated historical series are used to construct a reservoir inflows scenario tree. Other potential sources of uncertainty (e.g. load, failures, run-of-the-river generation, wind power, ...) are neglected in the model. Head and efficiency variations of hydroelectric plants are taken into account using concave and piecewise linear functions. The PHA is used to solve the resulting multistage stochastic linear program (MSLP).

The remainder of the paper is organized as follow. The mathematical formulation for the MGSP is presented in Section 2. Section 3 presents the PHA used to solve this problem. Section 4 describes a case study based on Hydro-Québec’s power system. Numerical results are presented in Section 5. Comments and conclusions are drawn in Section 6.

## 2. Midterm generation scheduling problem

### 2.1. Problem description

We consider a power system composed of hydro plants  $i \in I$  connected to reservoirs  $j \in J$ . The electrical load  $d_{zc}^t$  (MW) to be satisfied at all time periods  $t \in \mathcal{T} = \{1, 2, \dots, T\}$  is distributed in each zone  $z \in Z$  of a transmission network  $G = (Z, L)$ . Transmission links  $\ell \in L$  allow energy transfer between neighboring zones in the network. Short-term (hourly, daily) load variations within any given time period  $t \in \mathcal{T}$  are represented using a discretized load duration curve. Each load level  $c \in C$  has an associated duration  $\Delta t_c$  (h). Fig. 2 shows an example of load duration curve with three load levels.

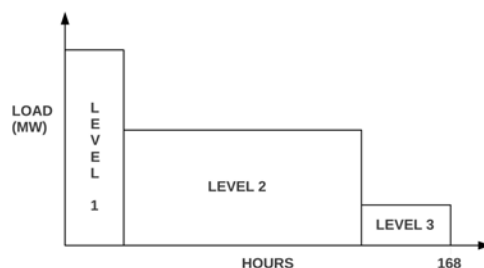


Figure 2: Example of a discretized load duration curve.

The objective function to be maximized is

$$\mathbb{E} \left[ \sum_{j \in J} \mathcal{R}_j(v_T^j) - M \sum_{t \in \mathcal{T}} \sum_{c \in \mathcal{C}} \sum_{z \in \mathcal{Z}} (\sigma_{zc}^t + \delta_{zc}^t) \middle| \mathcal{I}_1 \right] \quad (1)$$

where  $\mathbb{E}[\cdot | \cdot]$  is the conditional expectation operator and  $\mathcal{I}_1$  ( $\text{hm}^3$ ) is the inflow vector at the first period. We assume that the realization of  $\mathcal{I}_1$  is revealed to the decision maker at the beginning of the first period. The reward  $\mathcal{R}_j$  (\$) for reservoirs  $j \in J$  are concave and piecewise linear functions of the storage  $v_T^j$  ( $\text{hm}^3$ ) at the end of period  $t = T$ . The constant  $M > 0$  is used to penalize surplus  $\sigma_{zc}^t$  and shortages  $\delta_{zc}^t$  which are the slack variables in the energy budget equality constraints

$$\sum_{i \in I(z)} P_{ic}^t + \sum_{\ell \in L_+(z)} (1 - \epsilon_\ell) X_{\ell c}^t - \sum_{\ell \in L_-(z)} X_{\ell c}^t - \sigma_{zc}^t + \delta_{zc}^t = d_{zc}^t \quad (2)$$

for each load level  $c$ , time period  $t$  and zone  $z$ . Decision variables  $P_{ic}^t$  (MW) and  $X_{\ell c}^t$  (MW) represents the power output of hydro plant  $i$  and power flow on transmission link  $\ell$  respectively. The set  $I(z)$  contains hydro plants connected to zone  $z$ . Sets  $L_+(z) \subseteq L$  and  $L_-(z) \subseteq L$  contain transmission links entering and going out of zone  $z$  respectively. Parameter  $\epsilon_\ell$  represents the loss coefficient of links  $\ell$ .

Hydroelectricity generation constraints

$$P_{ic}^t \leq \phi_i^t(q_{ic}^t, \bar{v}_{j(i)}^t, \bar{v}_{\nu(i)}^t), \quad \forall i, c, t \quad (3)$$

ensure that hydro plants power output  $P_{ic}^t$  (MW) is upper bounded by a generation function  $\phi_i^t$  (MW) which depends the turbined outflow  $q_{ic}^t$  ( $\text{m}^3 \text{s}^{-1}$ ) and average storage  $\bar{v}_{j(i)}^t$  and  $\bar{v}_{\nu(i)}^t$  during period  $t$  in the upstream reservoir  $j(i)$  and downstream reservoir  $\nu(i)$ . Generation functions are concave and piecewise linear. Constraints

$$q_{ic}^t \leq \alpha_0^i + \alpha_1^i \bar{v}_{j(i)}^t + \alpha_2^i \bar{v}_{\nu(i)}^t, \quad \forall i, c, t \quad (4)$$

represents the variations of maximal turbined outflow as a function of reservoir storage.  $\alpha_0^i$ ,  $\alpha_1^i$  and  $\alpha_2^i$  are known constants.

Reservoir storage evolves from a known initial condition  $v_0^j$  according to discrete-time continuity equation

$$v_t^j = v_{t-1}^j - Q_t^{j,out} + Q_t^{j,in} + \mathcal{I}_t^j, \quad \forall j, t. \quad (5)$$

where  $v_t^j$  ( $\text{hm}^3$ ) represents storage of reservoir  $j$  at the end of period  $t$ . The controlled outflow volume for reservoir  $j$  outlet is defined by

$$Q_t^{j,out} := \sum_{c \in \mathcal{C}} \sum_{i \in I(j)} (D_{ic}^t + q_{ic}^t) \beta \Delta t_c \quad (\text{hm}^3)$$

where  $I(j)$  is the set of hydro plants connected to reservoir  $j$ ,  $D_{ic}^t$  ( $\text{m}^3 \text{s}^{-1}$ ) is the spillage,  $q_{ic}^t$  ( $\text{m}^3 \text{s}^{-1}$ ) is the turbined outflow and  $\beta = 0.0036$  is a constant for unit conversion. The controlled inflow for reservoir  $j$  is defined by

$$Q_t^{j,in} := \sum_{u \in \mathcal{U}(j)} Q_t^{u,out}$$

where the set  $\mathcal{U}(j)$  contains reservoirs located upstream of reservoir  $j$ . Natural inflow  $\mathcal{I}_t^j$  ( $\text{m}^3 \text{s}^{-1}$ ) are the only random parameters for this problem.

The following bounds

$$0 \leq P_{ic}^t \leq P_{it}^{\max}, \quad \forall i, c, t \quad (6)$$

$$q_{it}^{\min} \leq q_{ic}^t \leq q_{it}^{\max}, \quad \forall i, c, t \quad (7)$$

$$D_{it}^{\min} \leq D_{ic}^t \leq D_{it}^{\max}, \quad \forall i, c, t \quad (8)$$

$$v_{jt}^{\min} \leq v_t^j \leq v_{jt}^{\max}, \quad \forall j, t \quad (9)$$

$$0 \leq X_{lc}^t \leq X_{lt}^{\max}, \quad \forall l, t \quad (10)$$

$$0 \leq \sigma_{zc}^t, \delta_{zc}^t, \quad \forall z, c, t \quad (11)$$

are imposed on decision variables to represent physical limits, operational constraint or experience-based restrictions.

## 2.2. Inflow scenario tree

We assume that reservoir inflows vectors  $\mathcal{I}_t = (\mathcal{I}_t^j)$  ( $\text{hm}^3$ ) at time periods  $t \in \mathcal{T} = \{1, 2, \dots, T\}$  are discretely distributed and that their joint distribution has a finite number of possible outcomes. The stochastic process  $\{\mathcal{I}_t : t \in \mathcal{T}\}$  is modeled by a finite scenario tree. Tree nodes  $n \in \mathcal{N}$  represent every possible state of the stochastic process at all time periods. Each possible scenario (realization)  $\omega \in \Omega$  of the stochastic process corresponds to a path from the root  $0 \in \mathcal{N}$  to a leaf  $f(\omega) \in \mathcal{N}$  in the tree. An inflow vector  $\mathcal{I}_n$  is defined at each tree node. A simple example of a scenario tree with  $\mathcal{N} = \{0, 1, 2, 3, 4, 5, 6\}$  is presented in Fig. 3. In this example, scenario  $\omega = 1$  corresponds to the path 0-1-3.

## 2.3. Mathematical formulation

The problem (1)–(11) can be written

$$(\mathcal{P}) \quad \max \left\{ \sum_{n \in \mathcal{N}} p_n F_{t(n)}(\hat{x}_n) : \hat{x}_n \in \hat{X}_{t(n)}, \forall n \right\}$$

where node-wise control vectors

$$\hat{x}_n := (v_t^j, q_{ic}^t, P_{ic}^t, D_{ic}^t, X_{lc}^t, \sigma_{zc}^t, \delta_{zc}^t)$$

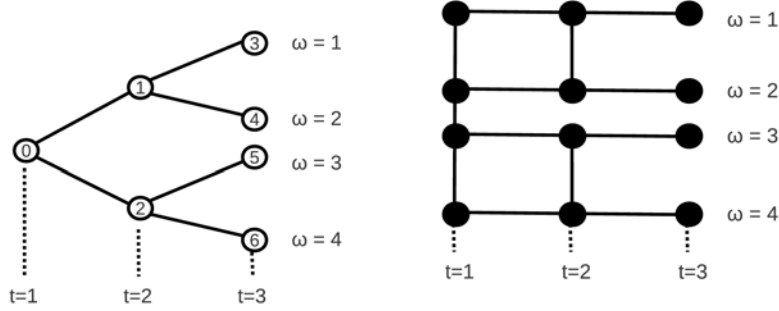


Figure 3: Example of node-wise (left) and scenario-wise (right) representations of a scenario tree.

defined at each tree node  $n$  contain all the decision variables required to operate the power system during one time period,  $p_n$  and  $t(n)$  is the probability and time period associated with node  $n$  (respectively),  $F_t$  are piecewise linear functions representing each term in the objective (1),  $\hat{X}_t$  is a polyhedral set defined by physical constraints (2)–(11) at period  $t$ .

To apply the scenario decomposition method on  $\mathcal{P}$ , we apply the following variable change. Node-wise control vectors  $\hat{x}_n$  at nodes  $n \in \mathcal{N}$  are replaced by scenario-wise control vectors  $x_{t\omega}$  at the corresponding time period  $t$  and scenario  $\omega$  in the tree. The resulting (equivalent) mathematical program is

$$(\mathcal{M}) \max \left\{ \sum_{\omega \in \Omega} p_\omega \sum_{t \in \mathcal{T}} F_t(x_{t\omega}) : x_{t\omega} \in X_{t\omega} \cap \mathcal{F}_{n(\omega,t)}, \forall t, \omega \right\}$$

where  $n(\omega, t)$  is the node corresponding to time period  $t$  and scenario  $\omega$ . Each set  $X_{t\omega}$  is defined by physical constraints (1)–(11) associated with inflow scenario  $\omega$  at time period  $t$ . The sets  $\mathcal{F}_n$  associated with tree nodes  $n \in \mathcal{N}$  is defined by non-anticipativity constraints

$$x_{t\omega} - \hat{x}_n = 0. \quad (12)$$

These constraints ensure that control vectors  $x_{t\omega}$  are scenario invariant at every tree node. Vectors  $\lambda_{n\omega}$  contains the dual variables associated with non-anticipativity constraints.

### 3. Solution method

#### 3.1. Scenario decomposition

The constraint matrix of  $\mathcal{M}$  is sparse and exhibits a special structure which can be exploited efficiently using a scenario decomposition method. As shown in Fig. 4, physical constraints (2)–(11) corresponds to small separate blocks containing nonzero coefficients in the constraints matrix. Each of these blocks is associated to a particular scenario  $\omega \in \Omega$  in the tree. Non-anticipativity constraints (12) corresponds to a large block with nonzero coefficients. Remaining matrix coefficients are equal to zero. Physical constraints are relatively

easy to deal with since they correspond to a set of independent blocks in the constraint matrix. Conversely, non-anticipativity constraints are more difficult since they couple scenario blocks to one another.

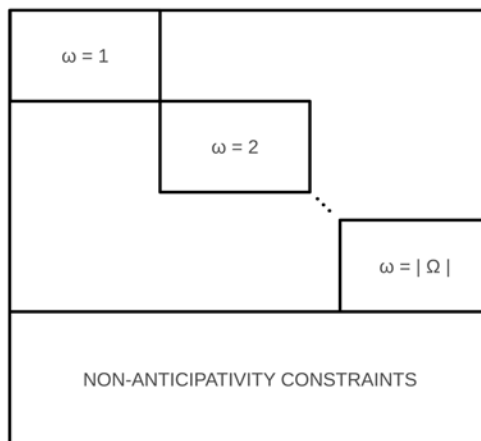


Figure 4: Structure of the constraints matrix.

In order to solve  $\mathcal{M}$  using the PHA, we apply Lagrangean relaxation on non-anticipativity constraints and penalize quadratically any violation of it. The resulting augmented Lagrangian is

$$\mathcal{A}_\rho(x, \hat{x}, \lambda) = \sum_{\omega \in \Omega} p_\omega \sum_{t \in \mathcal{T}} F_t(x_{t\omega}) - \sum_{\omega \in \Omega} \sum_{n \in \mathcal{N}(\omega)} \left( \lambda_{n\omega}^T (x_{t(n)\omega} - \hat{x}_n) + \frac{\rho}{2} \|x_{t(n)\omega} - \hat{x}_n\|_2^2 \right)$$

where  $\rho > 0$  is the penalty parameter,  $x = (x_{t\omega})$  is the scenario-wise solution,  $\hat{x} = (\hat{x}_n)$  is the node-wise solution,  $\lambda = (\lambda_{n\omega})$  is the dual vector associated with non-anticipativity constraints and  $\mathcal{N}(\omega)$  contains nodes visited by scenario  $\omega$ . All vectors are column-vectors and the operator  $(\cdot)^T$  represents the transpose.

### 3.2. Progressive hedging algorithm

The PHA is initialized with an estimation of  $\hat{x}^0$  and  $\lambda^0$ . At each iteration  $k = 0, 1, 2, \dots$  of the algorithm, two steps are performed:

**Step 1.** Find a new scenario-wise solution  $x^{k+1} = (x_{t\omega}^{k+1})$  by maximizing  $\mathcal{A}_{\rho^k}(x, \hat{x}^k, \lambda^k)$  for  $x \in X_{t\omega}$  using the current  $\hat{x}^k$  and  $\lambda^k$ . This large optimization problem can be decomposed

into much smaller scenario subproblems

$$(\mathcal{S}_\omega^k) \max_{x \in X(\omega)} p_\omega \sum_{t \in \mathcal{T}} F_t(x_{t\omega}) - \sum_{n \in \mathcal{N}(\omega)} \left( (\lambda_{n\omega}^k)^T (x_{t(n)\omega} - \hat{x}_n^k) + \frac{\rho}{2} \|x_{t(n)\omega} - \hat{x}_n^k\|_2^2 \right)$$

where  $X(\omega)$  is defined by physical constraints (2)–(11) associated with scenario  $\omega$ . Each subproblem  $\mathcal{S}_\omega^k$  corresponds to a deterministic version of  $\mathcal{M}$  to which linear and quadratic penalty terms are added. Subproblems can be solved sequentially or in parallel.

**Step 2.** Update node-wise control vectors by averaging scenario-wise control vectors using

$$\hat{x}_n^{k+1} \leftarrow \sum_{\omega \in \Omega(n)} p_\omega x_{t(n)\omega}^{k+1} / p_n, \quad \forall n$$

where  $\Omega(n) \subseteq \Omega$  contains all scenarios visiting node  $n$ . Update dual vectors

$$\lambda_{n\omega}^{k+1} \leftarrow \lambda_{n\omega}^k + \rho \left( x_{t(n)\omega}^{k+1} - \hat{x}_n^{k+1} \right), \quad \forall n, \omega.$$

Verify if the two following stopping conditions

$$\zeta_k := \frac{1}{T} \sum_{\omega \in \Omega} p_\omega \sum_{t \in \mathcal{T}} \|x_{t\omega}^{k+1} - \hat{x}_{n(t,\omega)}^{k+1}\|_2^2 < \tilde{\epsilon}_0 \quad (13)$$

$$\xi_k := \frac{|\mathcal{A}_\rho(x^{k+1}, \hat{x}^{k+1}, \lambda^{k+1}) - \mathcal{A}_\rho(x^k, \hat{x}^k, \lambda^k)|}{\mathcal{A}_\rho(x^k, \hat{x}^k, \lambda^k)} < \tilde{\epsilon}_1 \quad (14)$$

are satisfied for some stopping criteria  $\tilde{\epsilon}_0, \tilde{\epsilon}_1 > 0$ . Parameters  $\zeta_k$  and  $\xi_k$  measure violation of non-anticipativity constraints and the relative improvement of the augmented Lagrangian at the current iteration  $k$ . If the solution does not satisfy conditions (13) and (14), return to step 1.

Physical constraints are satisfied at each iteration since they are treated directly in  $\mathcal{S}_\omega^k$ . However, non-anticipativity constraints are expected to be violated in early iterations since these constraints are treated indirectly by penalizing violations. Linear and quadratic penalty terms in  $\mathcal{S}_\omega^k$  will ensure that the violation of non-anticipativity constraints will decrease gradually through the iterative process in order to obtain a feasible (non-anticipative) solution. The PHA is an exact method for  $\mathcal{M}$  since this problem is linear (and convex). A proof of convergence is presented in Rockafellar and Wets [22].

### 3.3. Penalty parameter update

The penalty parameter  $\rho$  weights quadratic penalties in  $\mathcal{S}_\omega^k$  and corresponds to step size in dual vectors update formulas. This parameter plays a key role by controlling the rate at which feasibility and the objective value are improved. In practice,  $\rho$  should be chosen carefully in order to make an optimal compromise between these two conflicting objectives. For large values of  $\rho$ , feasibility will improve rapidly, but refinement of the objective value might be slowed down. Conversely, a large number of iterations will be required to obtain a feasible solution if  $\rho$  is small.

Theoretical results presented in Rockafellar and Wets [22] are based on using a constant penalty parameter at each iteration. For practical applications, performance of the PHA might be enhanced by changing  $\rho_k$  at each iteration. In this study, the penalty parameter is initialized with some value  $\rho_0$  and updated using

$$\rho_{k+1} \leftarrow \mu \rho_k \quad (15)$$

which is the classical update formula for general augmented Lagrangian methods [25]. The rate at which  $\rho_k$  increases  $\mu \geq 1$  is a constant. Parameters  $\rho_0$  and  $\mu$  must be tuned in order to minimize the number of iterations to converge without sacrificing solution quality.

## 4. Numerical experiment

### 4.1. Power system

In this experiment, we consider a simplified version of HQ's generation scheduling problem for a  $T = 93$  weeks (periods) horizon, which begins on February 1<sup>st</sup>. Fig. 5 shows the simplified power system; it accounts for most of HQ power system storage and installed capacity. The simplified system contains 25 hydro plants and 21 reservoirs which accounts for most of HQ's power system storage and generation capacities. The total storage and generation capacities of the simplified system are 182 018 hm<sup>3</sup> (154 TWh) and 33.2 GW, respectively. The storage is 96 889 hm<sup>3</sup> at the beginning of the planning horizon.

The simplified transmission network contains 5 zones and 6 links. Table 4.1 shows the characteristics of the power system in each zone. Approximately half of the total storage and installed capacity is located with the La-Grande zone ( $z = 1$ ). About 43% of these quantities is located in the Churchill Falls ( $z = 2$ ) and Côte-Nord zones ( $z = 3$ ). The remaining storage and installed capacity is located in the Central zone ( $z = 4$ ). We assume no maintenance is scheduled. Therefore, all generation units are available at all time period. Piecewise linear generation functions for each hydro plant  $i$  are described using three hyperplanes. Reward functions  $R_j$  are described using 7 pieces. Shortage and surpluses are penalized using  $M = 10^{12}$ .

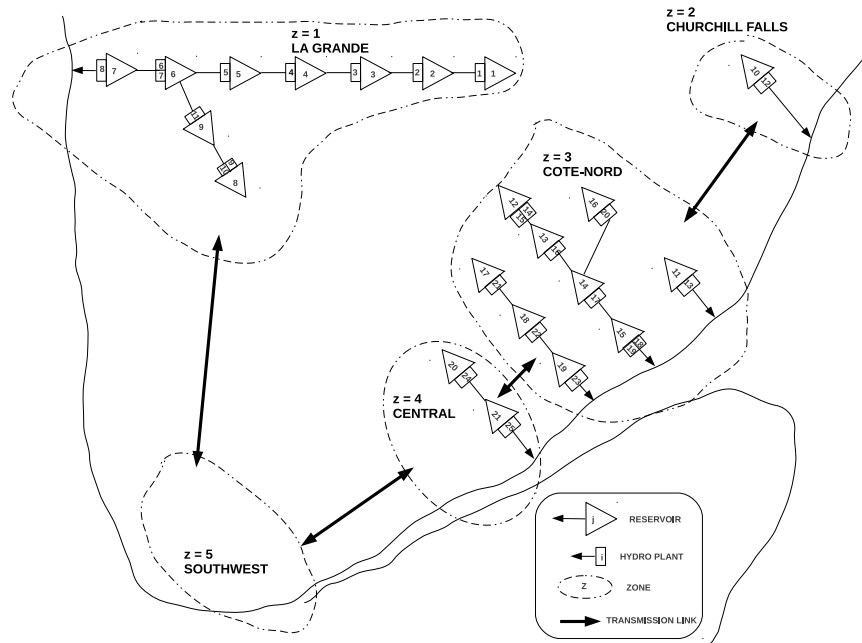


Figure 5: Simplified power system.

Table 1: Characteristics of each zone of the transmission network.

$z$	Load (TWh)	Installed capacity (GW)	Maximal storage ( $\text{hm}^3$ )
1	0.0	16.9	98 184
2	8.5	5.6	31 768
3	34.3	9.1	44 879
4	54.8	1.6	7 187
5	185.0	0	0

#### 4.2. Electrical load

The total electrical load to be satisfied is 282.6 TWh. Short-term (hourly, daily) variations of load at each period are represented with three levels. Fig. 6 shows variations of load intensity over the entire horizon for each level. The load is very high during winter and decreases importantly during summer and fall. The energy load is distributed in zones 2, 3, 4 and 5 of the transmission network as follow. 65% of the total load is located in the Southwest zone ( $z = 5$ ). 19% of the total load located in the Central zone ( $z = 4$ ). The remaining load (16%) is located in the Churchill Falls and Côte-Nord zones.

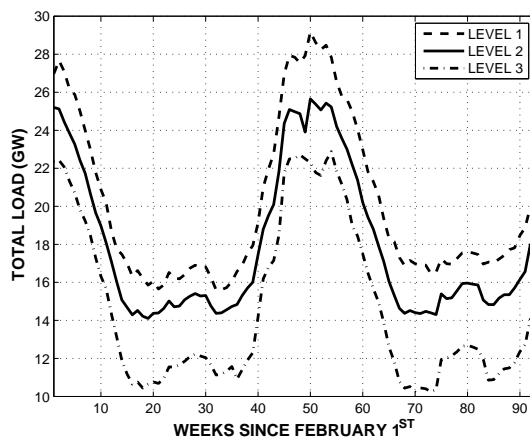


Figure 6: Variations of load levels over the planning horizon.

#### 4.3. Inflow scenario tree

Reservoir inflow variability is modeled using the scenario tree shown in Fig 7. The tree represents 16 inflow scenarios and contains 1019 nodes. The planning horizon is partitioned in four different sections. The first section corresponds to the winter season during which reservoir inflows is weak and identical for all scenarios. The second section corresponds to the springflood season. Four different outcomes are possible during this section depending on the springflood timing (early or late) and intensity (intense or weak). Summer and fall inflow variability is represented in the third section of the horizon. Finally, variability of the second year is represented in the fourth section.

Reservoir inflow series associated with each section is taken from the historical record. We assume that the occurrence probability of each scenario  $\omega \in \Omega$  is  $p_\omega = 1/16$ . The expected total inflow represented in the scenario tree is  $3.66 \times 10^5 \text{ hm}^3$  and exceeds the average historical inflow by 7.0%. The standard deviation of the total inflow represented in the scenario tree is  $2.46 \text{ hm}^3 \times 10^4 \text{ hm}^3$  and is smaller than the historical standard deviation of  $3.17 \text{ hm}^3 \times 10^4 \text{ hm}^3$ .

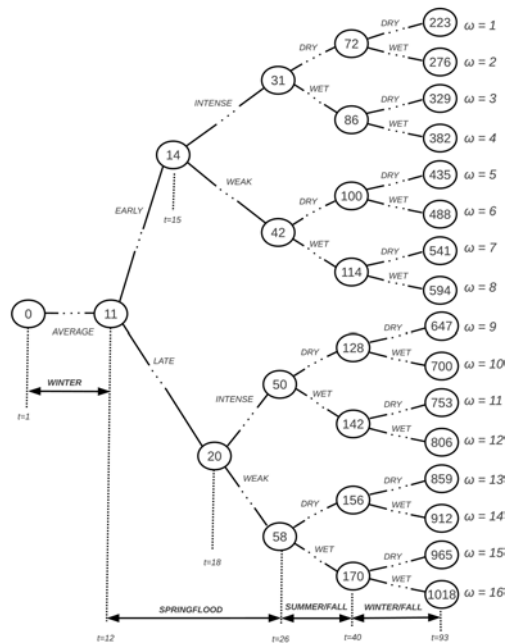


Figure 7: Scenario tree.

#### 4.4. Experimental set-up

The optimization problem is solved using a constant penalty parameter  $\rho \in [10^{-5}, 10^{-2}]$  and updating the penalty parameter using (15) with  $\mu \in [1.05, 1.60]$  and  $\rho_0 \in [10^{-7}, 10^{-5}]$ . The following stopping criteria  $\tilde{\epsilon}_0 = 10^{-2}$  and  $\tilde{\epsilon}_1 = 10^{-5}$  and used.

The PHA is implemented in C++ using version 12.4 of ILOG Concert technology library. Quadratic subproblems are solved sequentially using CPLEX barrier solver in parallel mode. Each quadratic subproblems has 33,244 decision variable and 37,275 linear constraints. All the computational results described in this section are obtained using a personal computer running on Ubuntu 12.04 64 bits with AMD Phenom II X6 2.8 GHz processor and 6 GB of RAM.

## 5. Results

### 5.1. Constant penalty parameter

Tables 2 summarize results obtained using a constant penalty parameter. According to our results, a compromise must be made between running time of the algorithm and the quality of the solution. Using a large penalty parameter increases convergence rate, but leads to a lower objective value. Using  $\rho = 10^{-2}$  converged rapidly after 65 iterations, but lead to a poor solution. Reasonable solutions were obtained using  $\rho \in [10^{-3}, 10^{-5}]$ .

Fig. 8 shows the algorithm's progress at each iteration when a constant penalty parameter is used. Stopping condition (13) was met before (14) for all  $\rho$  values used. Violation of non-anticipativity constraints is large initially ( $\zeta_1 \approx 3 \times 10^5$ ), but decreases rapidly in the

Table 2: Computational performance measures of the PHA using a constant penalty parameter.

$\rho$	Iterations	Time (min)	Objective ( $\times 10^9 \$$ )
$10^{-2}$	65	97.0	5.476984
$10^{-3}$	151	214.8	5.593470
$10^{-4}$	157	241.9	5.600270
$10^{-5}$	207	321.5	5.600546

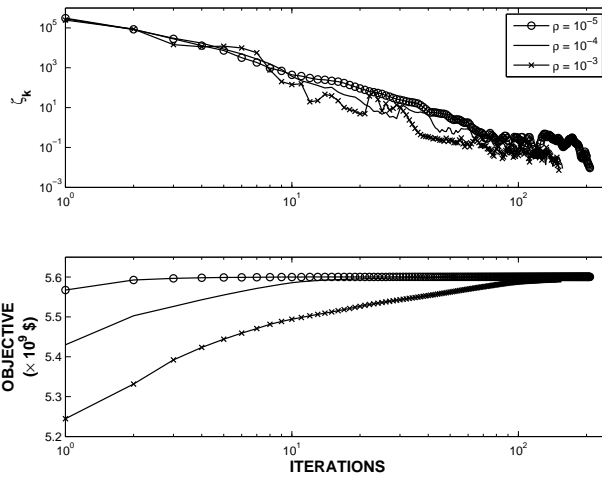


Figure 8: Convergence with a constant penalty parameter.

first 10–12 iterations. Slower progress is observed afterwards.

### 5.2. Variable penalty parameter

Computational results obtained using a variable penalty parameter are reported in Table 3. The algorithm converged to a high quality solution after 21–84 iterations depending on which  $\rho_0$  and  $\mu$  were used. In general, using large values of  $\rho_0$  and  $\mu$  reduces the number of iterations, but decreases solution quality.

Table 3: Computational performance measures of the PHA using a variable penalty parameter.

$\rho_0$	$\mu$	Iterations	Time (min)	Objective ( $\times 10^9$ \$)
$10^{-5}$	1.05	55	84.1	5.600317
$10^{-5}$	1.10	36	55.1	5.600059
$10^{-5}$	1.20	27	41.3	5.599254
$10^{-5}$	1.30	22	33.6	5.598417
$10^{-5}$	1.40	21	32.1	5.597551
$10^{-6}$	1.05	84	130.5	5.600545
$10^{-6}$	1.10	55	85.0	5.600528
$10^{-6}$	1.20	38	57.9	5.600476
$10^{-6}$	1.30	33	50.5	5.600421
$10^{-6}$	1.40	28	42.6	5.600361
$10^{-6}$	1.50	23	35.2	5.600298
$10^{-6}$	1.60	22	34.9	5.600239
$10^{-7}$	1.10	81	126.9	5.600547
$10^{-7}$	1.20	50	80.3	5.600531
$10^{-7}$	1.30	43	65.9	5.600502
$10^{-7}$	1.40	34	52.7	5.600460
$10^{-7}$	1.50	29	44.3	5.600419
$10^{-7}$	1.60	27	42.7	5.600373

The rate of progress obtained using a variable penalty parameter is shown in Figs. 9–11. Stopping condition (13) is met before (14) no matter which  $\rho_0$  and  $\mu$  values are used. Initially,  $\zeta_1$  is between  $3 \times 10^5$  and  $6 \times 10^5$ . The initial objective value varied between  $5.56744 \times 10^9$  \$ and  $5.60168 \times 10^9$  \$ for  $\rho_0 = 10^{-5}$  and  $\rho = 10^{-7}$ , respectively. Feasibility improved rapidly when large values of  $\rho_0$  were used, but converged to a lower objective value. The value of  $\mu$  influenced importantly the rate at which feasibility improved. The higher is  $\mu$ , the higher is the rate of improvement. In general, using  $\mu > 1$  was definitely beneficial.

## 6. Conclusions

In this study, a stochastic optimization model was proposed and evaluated for solving Hydro-Québec’s the midterm hydro generation scheduling problem (MGSP) under inflow

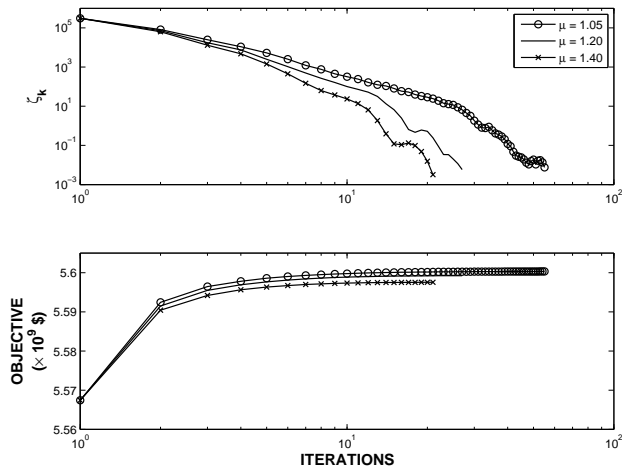


Figure 9: Convergence with a variable penalty parameter using  $\rho_0 = 10^{-5}$ .

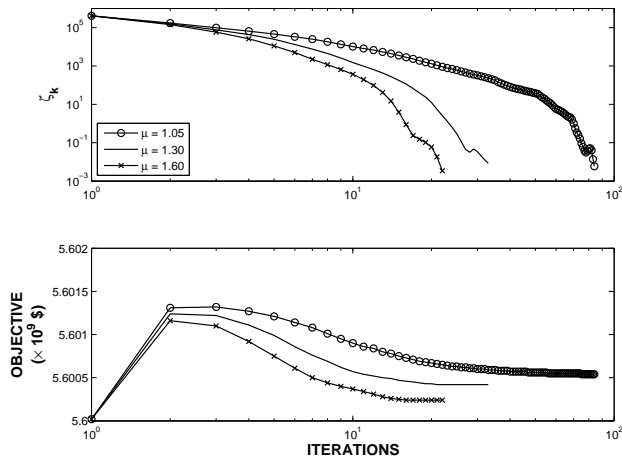


Figure 10: Convergence with a variable penalty parameter using  $\rho_0 = 10^{-6}$ .

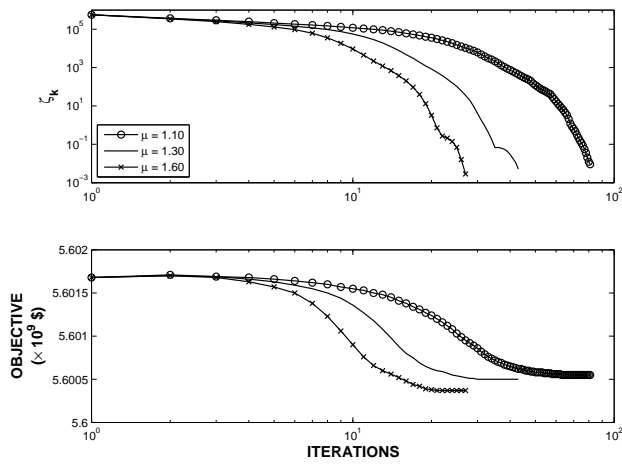


Figure 11: Convergence with a variable penalty parameter using  $\rho_0 = 10^{-7}$ .

uncertainty. A scenario tree based was used to model reservoir inflows variability. We applied the progressive hedging algorithm (PHA) to solve this problem. The proposed model was tested by performing a numerical experiment based on a simplified version of Hydro-Québec's generation scheduling problem. Computational results have shown that the number of iterations required to converge is quite sensitive the choice of penalty parameter. Updating the penalty parameter was required to obtain a high quality solution in reasonable running time.

## Appendix A. Notations

### Decision variables

$D_{ic}^t$	spilled release of plant $i$ at period $t$ for level $c$ ( $\text{m}^3 \text{s}^{-1}$ )
$q_{ic}^t$	turbined release of plant $i$ at period $t$ for level $c$ ( $\text{m}^3 \text{s}^{-1}$ )
$P_{ic}^t$	hydro generation of plant $i$ at period $t$ for level $c$ (MW)
$v_t^j$	storage of reservoir $j$ at the end of period $t$ ( $\text{hm}^3$ )
$X_{\ell c}^t$	transfer on link $\ell$ at period $t$ for level $c$ (MW)

### Sets

$I$	hydro plants
$I(j)$	hydro plants connected to reservoir $j$
$I(z)$	hydro plants in zone $z$
$J$	reservoirs
$L$	transmission links
$L_+(z)$	transmission links entering zone $z$
$L_-(z)$	transmission links outgoing zone $z$
$\mathcal{T}$	time periods
$\mathcal{U}(j)$	upstream reservoirs of reservoir $j$
$\mathcal{N}$	tree nodes

### Functions

$\mathcal{R}_j$	Reward for reservoir $j$ . (\$)
$j(i)$	upstream reservoir for plant $i$
$\nu(i)$	downstream reservoir for plant $i$

### Indexes

$j$	reservoir
$t$	time period
$u$	upstream reservoir
$c$	load level
$i$	hydro plant
$\ell$	transmission link
$n$	tree node

*Parameters*

$\mathcal{I}_t^j$	Inflow in reservoir $j$ at period $t$ ( $\text{hm}^3$ )
$d_{zc}^t$	Load in zone $z$ , for level $c$ at period $t$ (MW)
$T$	number of time periods
$\epsilon_\ell$	loss coefficient for link $\ell$
$\Delta t_c$	Duration associated with load level $c$ (hours)

**References**

- [1] Rani D, Moreira MM. Simulation-optimization modeling: A survey and potential application in reservoir systems operation. *Water Resour Manag* 2010;24(6):1107–38.
- [2] Labadie JW. Optimal operation of multireservoir systems: State-of-the-art review. *J Water Resour Plan Manag* 2004;130(2):93–111.
- [3] Wurbs R. Reservoir-system simulation and optimization models. *J Water Resour Plan Manag* 1993;119(4):455–72.
- [4] Yeh WWG. Reservoir management and operations models: A state-of-the-art review. *Water Resour Res* 1985;21(12):1797–818.
- [5] Bellman R. *Dynamic programming*. Princeton: Princeton University Press; 1957.
- [6] Nandalal KDW, Bogardi JJ. *Dynamic Programming Based Operation of Reservoir: Applicability and Limits*. International Hydrology Series; Cambridge University Press; 2nd ed.; 2007.
- [7] Yakowitz S. *Dynamic programming applications in water resources*. *Water Resour Res* 1982;18(4):673–96.
- [8] Tejada-Guibert JA, Johnson SA, R SJ. The value of hydrologic information in stochastic dynamic programming models of a multireservoir system. *Water Resour Res* 1995;31(10):2571–9.
- [9] Powell WB. *Approximate Dynamic Programming : Solving the Curses of Dimensionality*. Wiley; 2nd ed.; 2011.
- [10] Turgeon A, Charbonneau R. An aggregation-diaggregation approach to long-term reservoir management. *Water Resour Res* 1998;34(12):3585–94.
- [11] Archibald TW, McKinnon KIM, Thomas LC. An aggregate stochastic dynamic programming model of multireservoir system. *Water Resour Res* 1997;33(2):333–40.
- [12] Bertsekas DP, Tsitsiklis JN. *Neuro-dynamic programming*. Belmont: Athena Scientific; 1996.
- [13] Castelletti A, de Rigo D, Rizzoli AE, Soncini-Sessa R, Weber E. Neuro-dynamic programming for designing water reservoir network management policies. *Control Eng Pract* 2007;15(8):1031–8.
- [14] Pereira MVF, Pinto LMVG. Multi-stage stochastic optimization applied to energy planning. *Math Program* 1991;52(1-3):359–75.
- [15] Homem-de-Mello T, de Matos V, Finardi EC. Sampling strategies and stopping criteria for stochastic dual dynamic programming: a case study in long-term hydrothermal scheduling. *Energy Syst* 2011;2(1):1–31.
- [16] Goor Q, Kelman R, Tilmant A. Optimal multipurpose-multireservoir operation model with variable productivity of hydropower plants. *J Water Resour Plan Manag* 2011;137(3):258–67.
- [17] Tilmant A, Kelman R. A stochastic approach to analyze trade-offs and risks associated with large-scale water resources systems. *Water Resour Res* 2007;43(6):1–11.
- [18] Tilmant A, Pinte D, Goor Q. Assessing marginal water values in multipurpose multireservoir systems via stochastic programming. *Water Resour Res* 2008;44:1–17.
- [19] Rotting T, Gjelsvik A. Stochastic dual dynamic programming for seasonal scheduling in the norwegian power system. *IEEE Trans Power Syst* 1992;7(1):273–9.
- [20] Archibald TW, Buchanan C, McKinnon KIM, Thomas LC. Nested benders decomposition and dynamic programming for reservoir optimization. *J Operat Res Soc* 1999;50(5):468–79.
- [21] Jacobs J, Freeman G, Grygier J, Morton D, Schultz G, Staschus K, et al. Socrates: A system for scheduling hydroelectric generation under uncertainty. *Ann Operat Res* 1995;59(1):99–133.

- [22] Rockafellar RT, Wets RJB. Scenarios and policy aggregation in optimization under uncertainty. *Math Operat Res* 1991;16(1):119–47.
- [23] dos Santos MLL, da Silva EL, Finardi EC, Gonçalves REC. Practical aspects in solving the medium-term operation planning problem of hydrothermal power systems by using the progressive hedging method. *Int J Electr Power Energy Syst* 2009;31(9):546–52.
- [24] Gonçalves REC, Finardi EC, da Silva EL. Applying different decomposition schemes using the progressive hedging algorithm to the operation planning problem of a hydrothermal system. *Electr Power Syst Res* 2011;83(1):19–27.
- [25] Nocedal J, Wright S. *Numerical Optimization*. Springer Series in Operations Research and Financial Engineering; New York: Springer; 2nd ed.; 2006.